Crystallographic Analysis of Transition State Mimics Bound to Penicillopepsin: Difluorostatine- and Difluorostatone-Containing Peptides†

Michael N. G. James,*,‡ Anita R. Sielecki,‡ Kotoko Hayakawa,‡ and Michael H. Gelb§

Medical Research Council of Canada Group in Protein Structure and Function, Department of Biochemistry, University of Alberta, Edmonton, Alberta, Canada T6G 2H7, and Departments of Chemistry and Biochemistry, University of Washington, Seattle, Washington 98195

Received November 7, 1991; Revised Manuscript Received January 28, 1992

ABSTRACT: Difluorostatine- and difluorostatone-containing peptides have been evaluated as potent inhibitors of penicillopepsin, a member of the aspartic proteinase family of enzymes. Isovaleryl-Val-Val-StaF_2NHCH$_3$ [StaF_2 = (*S*)-4-amino-2,2-difluoro-(*R*)-3-hydroxy-6-methylheptanoic acid] and isovaleryl-Val-Val-StoF_2NHCH$_3$ [StoF_2 = (*S*)-4-amino-2,2-difluoro-3-oxo-6-methylheptanoic acid] have measured K_i's of 10 $\times$ 10^{-9} and 1 $\times$ 10^{-9} M, respectively, with this fungal proteinase. The StoF_2-containing peptide binds 32-fold more tightly to the enzyme than the analogous peptide containing the non-fluorinated statine ethyl ester. Each compound was cocrystallized with penicillopepsin, intensity data were collected to 1.8-Å resolution, and the atomic coordinates were refined to an *R* factor (= $\sum||F_o| - |F_c||/\sum|F_o|$) of 0.131 for both complexes. The inhibitors bind in the active site of penicillopepsin in much the same fashion as do other statine-containing inhibitors of penicillopepsin analyzed earlier [James, M. N. G., Sielecki, A., Salituro, F., Rich, D. H., & Hofmann, T. (1982) *Proc. Natl. Acad. Sci. U.S.A. 79*, 6137–6141; James, M. N. G., Sielecki, A., & Hofmann, T. (1985) in *Aspartic Proteinases and their Inhibitors* (Kosta, V., Ed.) pp 163–177, Walter deGruyter, Berlin]. The (*R*)-3-hydroxyl group in StaF_2 binds between the active site carboxyl groups of Asp33 and Asp213, making hydrogen-bonding contacts to each one. The ketone functional group of the StoF_2 inhibitor is bound as a hydrated species, with the *gem*-diol situated between the two aspartic acid carboxyl groups in a manner similar to that predicted for the tetrahedral intermediate expected during the catalytic hydrolysis of a peptide bond [James, M. N. G., & Sielecki, A. (1985) *Biochemistry 24*, 3701–3713]. One hydrogen-bonding interaction from the "outer" hydroxyl group is made to $O^{\delta 1}$ of Asp33, and the "inner" hydroxyl group forms two hydrogen-bonding contacts, one to each of the carboxyl groups of Asp33 ($O^{\delta 2}$) and Asp213 ($O^{\delta 2}$). The only structural difference between the StaF_2 and StoF_2 inhibitors that accounts for the factor of 10 in their K_i's is the additional (*R*)-3-OH group on the tetrahedral sp^3 carbon atom of the hydrated StoF_2 inhibitor. The intermolecular interactions involving the fluorine atoms of each inhibitor are normal van der Waals contacts to one of the carboxyl oxygen atoms of Asp213 (F2–$O^{\delta 2}$ Asp213, 2.9 Å). The observed stereochemistry of the bound StoF_2 group in the active site of penicillopepsin has stimulated our reappraisal of the catalytic pathway for the aspartic proteinases. In the formation of the tetrahedral intermediate, we consider Asp213 as the general base, Asp33 acts as a general acid, and the nucleophile is the central water molecule, bound between the two carboxyl groups. The present proposal most closely resembles that of Suguna et al. [Suguna, K., Padlan, E. A., Smith, C. W., Carlson, W. D., & Davies, D. R. (1987) *Proc. Natl. Acad. Sci. U.S.A. 84*, 7009–7013].

Pepstatin is a naturally occurring, potent peptide inhibitor of aspartic proteinases (Morishima et al., 1970; Aoyagi et al., 1972). It contains the unusual amino acid statine (*S*)-4-amino-(*S*)-3-hydroxy-6-methylheptanoic acid (Figure 1a). The statine residue is an important contributor to the tight binding of pepstatin to porcine pepsin (4.5 $\times$ 10^{-11} M) (Kunimoto et al., 1974; Workman & Burkitt, 1979). It was suggested that the tight binding is a consequence of the fact that statine is a mimic of a tetrahedral transition state intermediate formed during the hydrolysis of peptide substrates (Marciniszyn et al., 1976; Marshall, 1976). High-resolution X-ray crystallographic analysis of a molecular complex between penicillopepsin and a pepstatin analogue, IvaValVal-StaOEt (Iva = isovaleryl, OEt = ethyl ester), showed that statine is indeed a good mimic of the tetrahedral transition state intermediate (James et al., 1982). The (*S*)-3-hydroxyl group binds between the two catalytic carboxyl groups Asp33 and Asp213 of penicillopepsin, forming hydrogen bonds to both of them. A comparable study was carried out on the complex of penicillopepsin with a second peptide of the same type, where the leucine-like side chain of the statine residue was replaced by a lysine-like side chain (James et al., 1985). The result of this side-chain substitution was a marked decrease in the dissociation constant (Rich et al., 1983). The 1.8-Å crystallographic analysis of this structure allowed the further characterization of the residues lining the S_1-binding pocket (James & Sielecki, 1987). The mode of binding of the two pepstatin analogues to penicillopepsin is very similar except for the presence of an additional hydrogen-bonded ion-pair interaction between the ϵ-NH_3^+ group of the lysine-like side chain of the inhibitor and the carboxylate group of Asp77, on the flap. The enhanced binding of the lysyl analogue is probably due to this additional electrostatic interaction. The structures of the molecular complexes were used as a basis on

† The Medical Research Council of Canada supported the work in Alberta. The National Institutes of Health Provided funds for the studies in Seattle [HL-35235 and NIH Career Development Award (GM-00562) to M.H.G.]. M.H.G. is a fellow of the Alfred P. Sloan Foundation (1991–1993).

* Author to whom correspondence should be addressed.
‡ University of Alberta.
§ University of Washington.

0006-2960/92/0431-3872$03.00/0 © 1992 American Chemical Society

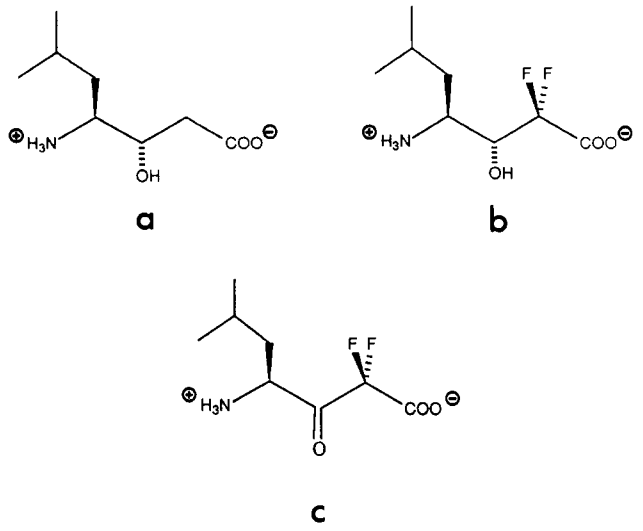

FIGURE 1: Molecular formulae for the statine (a), $StaF_2$ (b), and $StoF_2$ (c) groups.

which to develop a possible catalytic pathway for hydrolysis of good substrates by the aspartic proteinases (James & Sielecki, 1987; James & Sielecki, 1985).

Rich and co-workers have studied a class of pepsin inhibitors in which the (*S*)-3-hydroxyl group of the statine residue was oxidized to a ketone (Rich et al., 1982, 1984). This statone-containing peptide bound about 50-fold weaker than the analogous statine compound. Interestingly, ^{13}C-NMR studies revealed that the ketone of the enzyme-bound inhibitor was in the hydrated (*gem*-diol) state, suggesting that there exist favorable interactions between the hydrated ketone and the enzyme (Rich et al., 1982). We have described the preparation of peptides containing the difluorostatone ($StoF_2$)[1] residue (Gelb et al., 1985). The introduction of two fluorine atoms adjacent to the ketone (Figure 1c) promotes the hydration of the ketone, even in the absence of the enzyme. It was found that a peptide containing $StoF_2$ was about 20-fold more potent as an inhibitor of pepsin compared to the difluorostatine ($StaF_2$, Figure 1b) containing peptide and about 1000-fold more potent than the non-fluorinated statone-containing peptide (Gelb et al., 1985). Similar results were found with $StoF_2$ and $StaF_2$-containing peptides as inhibitors of human renin (Thaisrivongs et al., 1986; Fearon et al., 1987). It is likely that the hydrated difluorostatone closely resembles the structure of the tetrahedral intermediate formed during the hydrolysis of a peptide substrate.

The introduction of two fluorine atoms on the 2-carbon atom of statone provides an energetic advantage to inhibitor binding that is not available to the non-fluorinated statone group. This is because a component of the dissociation constant for the non-fluorinated statone peptide from the enzyme is the favorable dehydration of the unbound inhibitor from the hydrate to the ketone [the equilibrium constant for the hydration of the statone is 0.05 (Rich et al., 1985)]. In contrast, the $StoF_2$-containing peptide is not "pulled" off the enzyme by the mass action of dehydration since this polarized ketone prefers to be in the hydrated state both in solution and when bound to the enzyme (Gelb et al., 1985).

In order to elucidate the mode of binding of fluorinated statine and statone inhibitors of the aspartic proteinases, we have cocrystallized $IvaValValStaF_2NHCH_3$ and $IvaValValStoF_2NHCH_3$ with penicillopepsin and have solved and refined these molecular complexes at 1.8-Å resolution. A preliminary report on these results has been published (James et al., 1988). The resulting atomic coordinates of both complexes have been deposited with the Brookhaven Protein Data Bank (Bernstein et al., 1977).

Experimental Procedures

General Synthetic Procedures. Conditions for flash chromatography, HPLC, LSIMS, NMR, and TLC detection have been given previously (Fearon et al., 1987).

$StaF_2$ N-Methylamide Hydrochloride. *N*-BOC-$StaF_2$ ethyl ester [Fearon et al. (1987). 0.5 g, 1.47 mmol] was dissolved in 10 mL of methanol saturated with methylamine gas. After 2 h at room temperature, the solution was concentrated in vacuo to give an oil. To the residue was added 4 N HCl in dioxane (50 mL, prepared by passing a stream of anhydrous HCl gas through a flask of reagent-grade dioxane). After 30 min at room temperature, the solution was concentrated to a small volume in vacuo, and ether was added to give a gummy solid. The solid was triturated twice with ether, and the solid was dried in vacuo for several hours to yield the crude product (280 mg), which was used without further purification: NMR (D_2O, 80 MHz) δ 1.0 (br d, 6 H), 1.5–2.0 (br m, 3 H), 2.9 (s, 3 H), 3.6–3.8 (br m, 1 H), 4.1–4.3 (br m, 1 H).

N-BOC-Val-$StaF_2$ N-Methylamide. The compound from the previous step (280 mg, 1.07 mmol) and *N*-BOC-valine (Chemalog, 231 mg, 1.07 mmol) were dissolved in DMF (6.2 mL), and diethyl phosphorylcyanadate (Ikota et al., 1980) (Wako, 0.194 mL, 1.28 mmol) was added. The flask was stoppered and cooled in an ice bath. Triethylamine (0.312 mL, 2.24 mmol) was added, and the solution was stirred overnight at 4 °C. The mixture was concentrated in vacuo, and the residue was taken up in ethyl acetate, washed twice with 5% citric acid, once with 5% $NaHCO_3$, and once with brine. The organic layer was dried over $MgSO_4$, filtered, and concentrated in vacuo to give a crusty solid. The solid was recrystallized by dissolving it in a minimal amount of warm ethyl acetate followed by the addition of just enough low boiling petroleum to produce a slight cloudiness and finally cooling the solution on ice for 3 h. The solid was collected by filtration and washed with a small volume of ice-cold 10% ethyl acetate in petroleum ether to obtain 0.22 g of a white solid (mp 175–177 °C) TLC (100% ethyl acetate), R_f 0.8, detection with HCl/ninhydrin. NMR ($CDCl_3$, 300 MHz) δ 0.9 (br t 12 H), 1.5 (s, 9 H), 1.5–1.75 (m, 3 H), 2.15 (m, 1 H), 2.9 (d, 3 H), 3.7 (br t, 1 H), 4.1 (m, 2 H), 4.7 (d, 1 H), 5.0 (d, 1 H), 6.6 (d, 1 H), 7.15 (d, 1 H).

N-BOC-Val-Val-$StaF_2$ N-Methylamide. The compound from the previous step was treated with 4 N HCl in dioxane for 30 min at room temperature. Ether was added, and the solid was triturated with two portions of ether. The solid was dried in vacuo for several hours. The peptide hydrochloride (129 mg, 0.36 mmol), BOC-valine (78 mg, 0.36 mmol), and diethyl phosphorylcyanadate (Ikota et al., 1980) (65 μL, 0.43 mmol) were added to DMF (2 mL). After cooling on ice, triethylamine (105 μL, 0.76 mmol) was added, and the reaction was stirred on ice overnight. The reaction mixture was worked up as above. The solid obtained was recrystallized from ethyl acetate/petroleum ether as above to give 82 mg of a white solid. TLC (100% ethyl acetate) R_f 0.6, detected with Cl_2/tolidine. NMR ($CDCl_3$, 300 MHz) δ 0.90–1.1 (m, 18 H), 1.3 (s, 9 H), 1.4–1.6 (br m, 3 H), 2.3 (m, 2 H), 2.9 (d, 3 H), 3.9 (t, 1 H), 4.1–4.3 (m, 3 H), 4.7 (d, 1 H), 5.25 (d, 1 H), 6.75 (d, 1 H), 7.15 (d, 1 H), 7.4 (d, 1 H).

[1] Abbreviations: BOC, *tert*-butyloxycarbonyl; LSIMS, liquid secondary ion mass spectrometry; $StaF_2$, (*S*)-4-amino-2,2-difluoro-(*R*)-3-hydroxy-6-methylheptanoic acid; $StoF_2$, (*S*)-4-amino-2,2-difluoro-3-oxo-6-methylheptanoic acid.

Iva-Val-Val-StaF$_2$ N-Methylamide. The compound from the previous step was treated with 4 N HCl and triturated with ether as before. After drying in vacuo for several hours, 57 mg of the peptide hydrochloride as a white solid was obtained. This material (57 mg, 0.13 mmol) was dissolved in DMF (0.6 mL) and triethylamine (19 μL, 0.14 mmol), and isovaleric anhydride (0.5 mmol) was added. The isovaleric anhydride was prepared by adding a solution of isovaleric acid (Aldrich, 109 μL) in CH_2Cl_2 (0.5 mL) to a solution of dicyclohexylcarbodiimide (Aldrich, 104 mg) in CH_2Cl_2 (0.25 mL). After 1 h on ice and 30 min at −20 °C, the solution was filtered through a glass wool-plugged Pasteur pipet directly into the peptide reaction solution. After 1 h at room temperature, the reaction mixture solidified. After an additional 3 h, the solution was filtered with the aid of some ethyl acetate, and the solid was washed with ethyl acetate at room temperature. The solid was dried in vacuo to yield 60 mg of product which contained some triethylamine (as judged by NMR). The solid was dissolved in *n*-butanol/ethyl acetate (1:1) by gentle warming, and the solution was washed twice with 5% citric acid, once with 5% $NaHCO_3$, and once with brine. The organic phase was dried over $MgSO_4$. After filtration, the solution was concentrated in vacuo to give a white solid. The solid was recrystallized from ethyl acetate to give 40 mg of the pure product. TLC (10% methanol in $CHCl_3$) R_f 0.6, detected with Cl_2/tolidine. NMR ($CDCl_3$/DMSO, 300 MHz) δ 0.9–1.1 (br m, 24 H), 1.3–1.6 (br m, 3 H), 2.1–2.3 (br m, 5 H), 2.9 (d, 3 H), 4.0–4.3 (m, 4 H), 7.05 (d, 1 H), 7.12 (d, 1 H), 7.19 (d, 1 H), 7.57 (d, 1 H). LSIMS (calcd for $C_{24}H_{44}F_2N_4O_5$ + 1) 506, obsd 506.

Iva-Val-Val-StoF$_2$ N-Methylamide. The compound from the previous step (13 mg, 0.026 mmol) was dissolved in dry DMSO (217 μL) and dry toluene (217 μL). Both solvents were distilled from CaH under argon. Dicyclohexylcarbodiimide (33 mg, 0.158 mmol) was added, followed by dichloroacetic acid (1.3 μL, 0.016 mmol). The mixture was stirred overnight at room temperature in a stoppered flask. Oxalic acid in methanol (450 μL of a 0.35 M solution) was added, and the mixture was stirred for 10 min at room temperature. The solution was mixed with *n*-butanol/ethyl acetate (1:1) and washed once with 5% $NaHCO_3$ and once with brine. The organic phase was centrifuged to remove some solid dicyclohexylurea, and the supernatant was concentrated in vacuo. The product was first purified by flash chromatography on silica gel with 3% methanol in $CHCl_3$ followed by HPLC on a preparative reverse-phase C_{18} column with CH_3CN/H_2O (2.5:1 v/v) to give 6 mg of pure product. TLC (10% methanol in $CHCl_3$) R_f 0.65, detected with Cl_2/tolidine. NMR ($CDCl_3$, 300 MHz) δ 0.9–1.1 (br m, 24 H), 1.5–1.8 (br m, 3 H), 1.9–2.2 (br m, 5 H), 2.9 (d, 3 H), 4.4–4.7 (m, 3 H), 7.4 (d, 1 H), 7.6 (d, 1 H), 8.2 (d, 1 H), 8.3 (d, 1 H). LSIMS (calcd for $C_{24}H_{42}F_2N_4O_5$ + 1) 504, obsd 504.

Determination of the K_i Values. Stock solutions of peptides were prepared in DMSO, and the concentrations were determined from the amino acid analyses using norvaline as a standard. Penicillopepsin was assayed with the colorimetric substrate acetyl-Ala-Ala-Lys-(NO_2)Phe-Ala-Ala-amide (obtained as a generous gift from Prof. Theo Hofmann, University of Toronto) by monitoring the absorbance at 277 nm in assay buffer (20 mM sodium acetate, 16.5 mM KCl, pH 4.5). Enzymatic velocities were calculated from the slopes of the absorbance vs time plots using the molar absorbance coefficient at 277 nm of 10970 M^{-1} cm^{-1} (Hofmann & Hodges, 1982). The K_m value for this substrate under the above conditions was measured to be 180 μM by fitting the plot of the observed initial velocities vs substrate concentrations to the Michaelis–Menten equation. The enzyme concentration in the assays was typically 1 nM. For the less-potent inhibitors, Iva-Val-Val-Sta-OEt (compound kindly supplied by D. Rich, University of Wisconsin) and Iva-Val-Val-StaF$_2$-NHMe, concentrations of inhibitor in the range of 10–50 nM were used, and K_i values of 32 ± 2 and 10 ± 1 nM were obtained, respectively. These values were obtained from the ratio of initial steady-state velocities in the presence and absence of inhibitor using the standard equation for competitive inhibition. For the more potent inhibitor, Iva–Val-Val-StoF$_2$-NHMe, the concentrations of inhibitor used (0.5–10 nM) were similar in magnitude to the enzyme concentration, and the steady-state velocity data were fit to an equation for competitive inhibition that takes into account the depletion of free inhibitor concentration due to enzyme binding [eq 21 of Morrison and Walsh (1988)]. In order to apply this equation, it is necessary to know accurately the enzyme concentration. This was accomplished by carrying out the colorimetric assay in the presence of about 10 nM enzyme and titrating the activity to zero with known amounts of Iva-Val-Val-StoF$_2$-NHMe. By using these methods, a K_i of 1 ± 0.2 nM was obtained. In all experiments with Iva-Val-Val-StaF$_2$-NHMe, a linear steady-state velocity was observed immediately after adding enzyme to a solution of substrate and inhibitor. With Iva-Val-Val-StoF$_2$-NHMe, a pre-steady-state phase was seen in which the enzymatic velocity decreased to a linear initial steady-state velocity over an initial period of 2–3 min. Such behavior has been observed with a variety of tight-binding inhibitors of aspartic proteinases (Rich, 1985; Bartlett & Kezer, 1984; Gelb et al., 1985). It is also typical of tight and slow binding as described by Morrison and Walsh (1988).

Table I: Crystal Data for Penicillopepsin and the StaF$_2$ and StoF$_2$ Inhibitor Cocrystals[a]

	penicillopepsin		
	native	+StaF$_2$	+StoF$_2$
space group	C2	C2	C2
a (Å)	97.4	97.6	97.5
b (Å)	46.6	46.6	46.6
c (Å)	65.4	66.4	66.2
β (deg)	115.4	116.1	116.0

[a] Crystallization conditions: 2.5 M Li_2SO_4 and 0.1 M $NaC_2H_3O_2$ buffer, pH 4.4. The relatively insoluble inhibitors were first dissolved in buffers containing 5% dimethylformamide in order to form the inhibited complex.

Crystallization and Structure Solution. Cocrystals of penicillopepsin with each of the statine-based inhibitors were grown as described previously (James et al., 1982; Table I). The external morphology of the crystals of the complexes was very different from that of the native crystals. Nonetheless, the space group and unit cell parameters for each of the derivative crystals indicated that they are reasonably isomorphous with crystals of native penicillopepsin (Table I).

X-ray intensity data were collected on an Enraf-Nonius CAD4 diffractometer with Ni-filtered Cu Kᾱ radiation to a resolution of 1.8 Å. The data were measured in shells of 2θ, collecting the highest resolution shell (2.0–1.8 Å) first. Data processing included the correction of the measured intensity values for X-ray decay (Hendrickson, 1976), absorption (North et al., 1968), geometrical factors (Lorentz and polarization), and the conversion to structure factor amplitudes, $|F_{complex}|$. Details of the data collection statistics are summarized in Table II.

From the crystal data in Table I it can be seen that there is a relatively large increase in the *c* axis length of ~1.5% and

Table II: Intensity Data Statistics for $StaF_2$ and $StoF_2$ Inhibitor Cocrystals

	$StaF_2$ + penpep	$StoF_2$ + penpep
total measured reflections (45.0–1.8 Å)	27895	27480
unique reflections	24987	24854
merging R_m[a] for data	0.031	0.037
isomorphous R_I[b] factor	0.323	0.263
decay:[c] $I_f/I_{t=0}$	0.93–0.72	0.95–0.76
maximum absorption correction	1.25	1.28

[a] $R_m = \sum(I_i - \bar{I})/\sum I_i$, where I_i are the intensities of multiple measured reflections and $\bar{I}$ is their average. [b] $R_I = \sum||F_{complex}| - |F_{native}||/\sum|F_{complex}|$, where $|F_{complex}|$ and $|F_{native}|$ are the complex and native structure factors amplitudes, respectively. [c] In addition to five standard reflections measured at regular intervals throughout the data collection, the set of initial ~1400 reflections were measured again at the end of the data collection to estimate the decay as a function of time and resolution (Hendrickson, 1976). The ratio of final to initial intensities given above correspond to the values at the minimum and maximum resolution ranges measured, respectively.

an increase in the β angle of the unit cell. We interpreted the large value of the isomorphous R_I factor for each complex (Table II) as due partly to the presence of the inhibitor and partly to the relative lack of isomorphism of the crystals. The change in the cell dimensions means that the molecular transform was not likely to be sampled at the same places as it was for the native crystals, so that the difference electron density map computed to show the inhibitor will be only partly correct. Clearly, extensive refinement against the measured structure factor amplitudes of the complexes was going to be required to obtain a reliable description of the enzyme–inhibitor binding interactions.

Difference electron density maps for both inhibitors were computed with coefficients $|F_{complex}| - |F_{native}|$ and calculated phases based on the refined native structure but computed omitting all solvent atoms in the region encompassing the active site. The "flap" region, residues 72–82, was included in the closed conformation found in the other previously solved complexes of statine analogues bound to penicillopepsin (James et al., 1982, 1985). These maps clearly showed continuous positive electron density for each inhibitor bound in the active site of penicillopepsin. A molecular model of each inhibitor was fitted to the electron density countours on an MMS-X interactive graphics computer (Barry et al., 1976) using the program M3 written by Colin Broughton in our laboratory (Sielecki et al., 1982). Initial atomic coordinates were derived and restrained-parameter least-squares refinement was initiated. The computer software used for the refinement was PROTIN/PROLSQ (Hendrickson & Konnert, 1981; Hendrickson, 1985).

Results and Discussion

The peptides $IvaValValStaF_2NHCH_3$ and $IvaValValStoF_2NHCH_3$ were prepared and evaluated as inhibitors of penicillopepsin as described under Experimental Procedures. These peptides are modified versions of a previously reported penicillopepsin inhibitor, IvaValValStaOEt (James et al., 1982). The replacement of the ethyl ester by the N-methyl amide was necessary to facilitate the synthesis of the fluorinated compounds. Difluorostatine ethyl ester is not stable because it readily cyclizes to form the lactam.

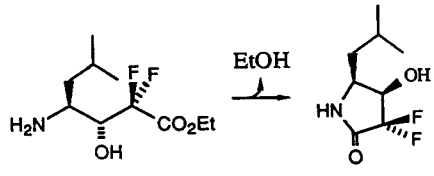

Table III: Restrained-Parameter, Least-Squares Refinement Statistics for $StaF_2$ and $StoF_2$ Complex Structures

	$StaF_2$ + penpep	$StoF_2$ + penpep
R factor ($= \sum||F_o| - |F_c||/\sum|F_o|$)[a]	0.131	0.131
resolution range (Å)	8.0–1.8	8.0–1.8
no. of reflections [$I \geq 1\sigma(I)$]	22464	22675
no. of protein atoms (+ sugars)[b]	2386	2386
no. of inhibitor atoms	35	36
no. of solvent molecules[b]	298	279
av temp factor, $\bar{B}$ (Å^2)	12.8	13.0
rms deviations from ideal values		
covalent bond distances (Å)	0.016	0.017
angle distances (Å)	0.043	0.038
planar 1–4 distances (Å)	0.044	0.039
planar group (Å)	0.008	0.010
chiral centers (Å^3)	0.195	0.203
nonbonded contact distances (Å)		
(a) single torsion (1–4)	0.24	0.24
(b) multiple torsion	0.18	0.18
(c) possible hydrogen bonds[c]	0.20	0.19
planar peptide group torsion angles	1.6°	2.1°

[a] $|F_o|$ and $|F_c|$ are the observed and calculated structure factor amplitudes, respectively. [b] In addition to refining the molecular complex of penicillopepsin and the two statine-based inhibitors, several new features of the penicillopepsin molecule itself have become apparent. Two *O*-linked sugar residues were discovered; an α-D-mannose on Ser3 O^{γ} and a tentatively assigned xylopyranose monosaccharide on Thr7 $O^{\gamma 1}$. In addition, a strongly bound solvent feature was reinterpreted as a sulfate anion, and an extensive revision of the strongly bound, highly ordered solvent structure was performed. Lastly, alternative side-chain conformations were detected for a number of residues. Details of these new features of penicillopepsin will be reserved for a separate paper that is in preparation. [c] No restraints were applied on possible hydrogen bonds when the distance between the atoms involved was larger than the sum of the corresponding van der Waals radii.

The K_i value for $IvaValValStoF_2NHCH_3$ is 1 ± 0.2 nM, 10-fold below that of $IvaValValStaF_2NHCH_3$ (K_i = 10 ± 1 nM). This difference in potencies is similar to the 20-fold difference in the K_i values for the $StoF_2$- and $StaF_2$-containing pepsin inhibitors (Gelb et al., 1985) and the 17-fold difference seen with analogous renin inhibitors (Fearon et al., 1987). A K_i value of 32 ± 2 nM was measured for the non-fluorinated peptide inhibitor IvaValValStaOEt. Since IvaValValStaOEt and the difluorinated inhibitors differ both in the presence of an ester versus an amide at their C-termini and in the substitution of fluorine atoms on the methylene group of the statine, it is not possible to associate these measured differences in K_i with a specific single functionality. Nevertheless, $IvaValValStoF_2NHCH_3$ is one of the most potent penicillopepsin inhibitors reported to date.

The crystallographic refinement data and statistics for the complexes of penicillopepsin with $IvaValValStaF_2NHCH_3$ and $IvaValValStoF_2NHCH_3$ are detailed in Table III. Perusal of this table shows that both molecular complexes have been refined to a satisfactory level within the limits of precision and resolution of the measured intensity data. The molecular models of each inhibitor fit the electron density distribution well, as can be judged from Figure 2. The hydrogen-bonding interactions at the active site carboxyl groups of Asp33 and Asp213 are confidently determined, as this region is very well ordered in each complex. The temperature factors (B) of the atoms of penicillopepsin in the active site region and of the $StaF_2$ and $StoF_2$ residues of the inhibitors range from 4 to 10 Å^2.

Figure 2b shows clearly that the carbonyl carbon atom of the $StoF_2$ residue is hydrated. There are two well-resolved peaks in the electron density map that accommodate the *gem*-diol. This is contrasted with the single (R)-3-hydroxyl peak present in the electron density map corresponding to the

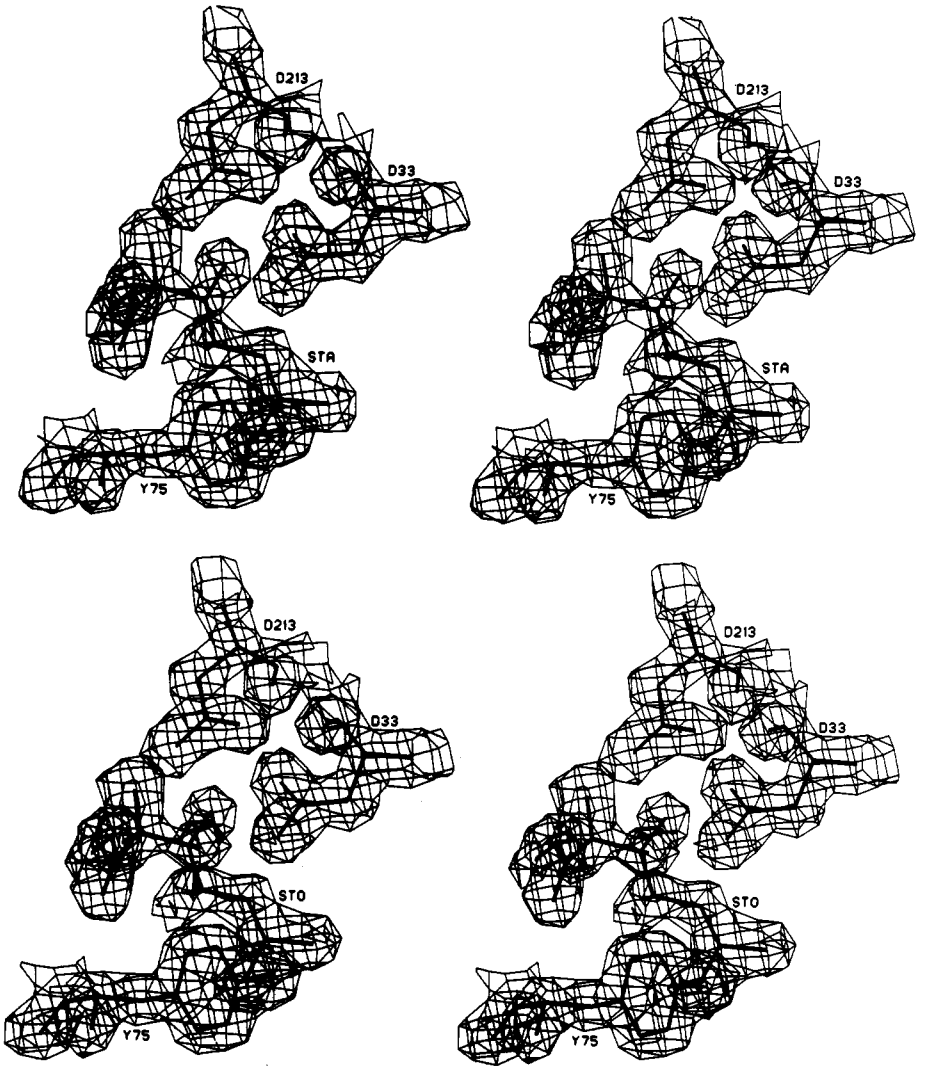

FIGURE 2: Electron density distributions of the final $(2|F_o| - |F_c|)\ \alpha_c$ maps in the immediate vicinity of the catalytic aspartic acid residues, Asp33 and Asp213. Tyr75, on the flap, is also depicted in the "closed" conformation that is stabilized by the binding of the inhibitors in the active site cleft. The contour level is 0.50 e/Å^3. (a, top) Difluorostatine complex. (b, bottom) Difluorostatone complex.

$StaF_2$ inhibitor (Figure 2a). The fluorine NMR spectrum of $IvaValValStoF_2NHCH_3$ in 80% DMSO/20% H_2O showed resonances only from the hydrated form. Thus, this peptide is fully hydrated both free in solution and in the complex with penicillopepsin. It is not clear from the present studies whether the *gem*-diol must first dehydrate to the ketone before binding to the enzyme or whether the *gem*-diol simply displaces the water molecule bound in native penicillopepsin (James & Sielecki, 1983).

Comparison of the Binding Modes of the $StaF_2$- and $StoF_2$-Containing Peptides to Penicillopepsin

The two inhibitors adopt virtually identical conformations in the active site of penicillopepsin (Figure 3). Superposition of the 35 common atoms of both inhibitors by a least-squares fitting program [LSQEM (W. Bennett)] results in a root mean square (rms) difference of 0.12 Å, a value that is similar in magnitude to the coordinate accuracy of atoms in the well ordered regions of the whole structure of the complex. The largest deviation (0.2 Å) occurs at the methyl group of the methyl amide.

In order to detect whether or not the two inhibitors are bound in the active site in exactly the same manner, the main-chain atoms of the penicillopepsin molecules of the two complexes were superimposed by the same least-squares procedure. The rms difference for the 1293 main-chain atoms was 0.09 Å, a value similar to that obtained for the atoms of the inhibitors alone. The orientation matrix that resulted from this superposition was then applied to the coordinates of the inhibitors. The comparison of the transformed inhibitor coordinates yielded an rms difference at 0.21 Å, nearly twice the value obtained when the inhibitor models were optimally overlapped by the least-squares procedure (0.12 Å). The regions of the inhibitor molecules that are positioned in a significantly different manner relative to the penicillopepsin active site are the $StaF_2NHCH_3$ and the $StoF_2NHCH_3$ parts. There are differences of up to 0.48 Å in this region (Figure 3). The differences must be due to the presence of the additional hydroxyl group in the hydrated form of $StoF_2$. The presence of the (*R*)-3-hydroxyl group causes the whole $StoF_2$ residue to be displaced farther from the Asp33 carboxylate relative to the position of the $StaF_2$ in the other complex (Figure 3). The displacement is 0.3 Å at the tetrahedral carbon atom of the $StaF_2$ ($StoF_2$) group.

Changes in the Penicillopepsin Native Structure Upon Inhibitor Binding

The binding of substrates or inhibitors to the active sites of enzymes is often accompanied by two energetically competing phenomena. The displacement of ordered water molecules from the enzyme surface is an entropically favorable process that leads to a lower free energy of the complex and

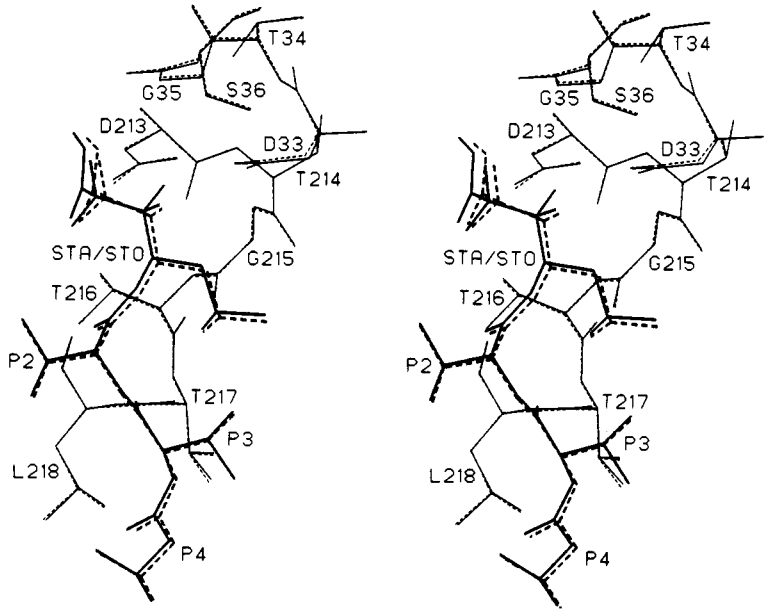

FIGURE 3: Difference in binding modes of the $StaF_2$ and $StoF_2$ inhibitors in the active site cleft. The coordinates of both complexes have been superposed using the orientation matrix that optimizes the fit of the 1293 main-chain atoms of the penicillopepsin molecule in each complex.

tighter binding. Movements of segments of polypeptide chain in the enzyme provide the most complementary interaction surface possible with the cognate molecule. These conformational changes are energetically unfavorable as they are often accompanied by a reduction in conformational entropy. Both phenomena are observed in the present complexes of penicillopepsin with the difluorostatine (one) containing inhibitors.

Since X-ray crystallography allows us to locate with confidence only the most highly ordered solvent molecules, it is difficult to provide an exact accounting of the number of solvent molecules displaced upon complex formation. A total of nine ordered water molecules are displaced from the active site region of penicillopepsin when either inhibitor is present. The displaced waters are O39, O61, O284, O170, O257, O241, O145, O160, and O300 (James & Sielecki, 1983). Three additional ordered water molecules in the native penicillopepsin structure, O70, O111, and O305 are displaced as a result of the movement of the residues of the flap (James et al., 1982). Lastly, eight ordered water molecules in the crystal structures of the inhibitor complexes occupy positions that correspond to the positions occupied by the residues of the flap in native uncomplexed penicillopepsin. The solvent structure associated with both inhibitor complexes is very similar within the limits of the structure determinations. There are only three relatively weakly ordered water molecules in the active site region that occupy different positions in the two complexes.

The region of penicillopepsin that undergoes the largest conformational change upon binding the $StaF_2$- and $StoF_2$-containing inhibitors is that part of the molecule known as the "flap". The flap of the aspartic proteinases is a β-hairpin loop that in penicillopepsin extends from Ser72 to Ser82. The conformational differences with the native enzyme can be described as an overall bending of this flap with a hinge between Ser72 and Ser82 so that these two residues are "fixed" and the tip of the loop, Gly76–Asp77, undergoes the largest change in position. The Cα atom of Gly76, in the structures of these and other inhibitor complexes, is $\sim$4 Å away from its position in the native enzyme (James et al., 1982, 1983).

Comparison of the coordinates of the 1257 main-chain atoms (omitting nine residues in the flap region) of native penicillopepsin with the equivalent atoms in the penicillopepsin

Table IV: Poorly Defined Residues in the Refined Structures of the Sta/Sto–Penicillopepsin Complexes

residues	comments
A1	weak density for α-NH_3^+
T9, S52, S67, S89 V155, S197, S202 Q237, S250, S257	two alternate side-chain conformations
D313	three alternate side-chain conformations
I18, Q133	poor fit of end of side chain to electron density—surface residue
K64, Q107	very weak density for side chain beyond C^γ
D206, N252	side-chain density discontinuous
S277–S281	very poor density for whole region ($B > 50$ Å^2)

structures of the two complexes gives root mean square (rms) agreement values of 0.26 and 0.23 Å for the $StaF_2$ and $StoF_2$ inhibitors, respectively. Apart from the flap region, the largest differences in conformation are observed in the relatively poorly ordered regions of the enzyme (Table IV). Before proceeding with this discussion, it should be emphasized that the atomic coordinate accuracy is directly related to the magnitude of the atomic thermal parameters, i.e., the larger the B factor, the larger will be the coordinate uncertainty. Thus, when comparing coordinates of atoms in very flexible or poorly ordered regions of proteins, one expects larger discrepancies in these regions. These discrepancies may have nothing to do with inhibitor binding but may just reflect the relative lack of order in that part of the protein.

As described for native penicillopepsin (James & Sielecki, 1983), there is only one loop, also in the complexes, that is significantly disordered, Ser277–Ser281 (Table IV). The temperature factors for the main-chain atoms of the five residues in this loop are greater than 50 Å^2 (Figure 4). The equivalent loop in most other aspartic proteinase crystal structures is also disordered. Other segments of contiguous residues exhibiting coordinate differences greater than 0.3 Å between the native and complexed conformations of penicillopepsin are Ala1–Ala2; Gln51-Gly53; Ile73–Ala81 in the flap region, a short helical region from Gln107 to Gln113, the external loop regions Gly177–Ser178 (native vs $StaF_2$ complex only). Asn186–Phe190, and Gly235–Gly244, and Gly292–

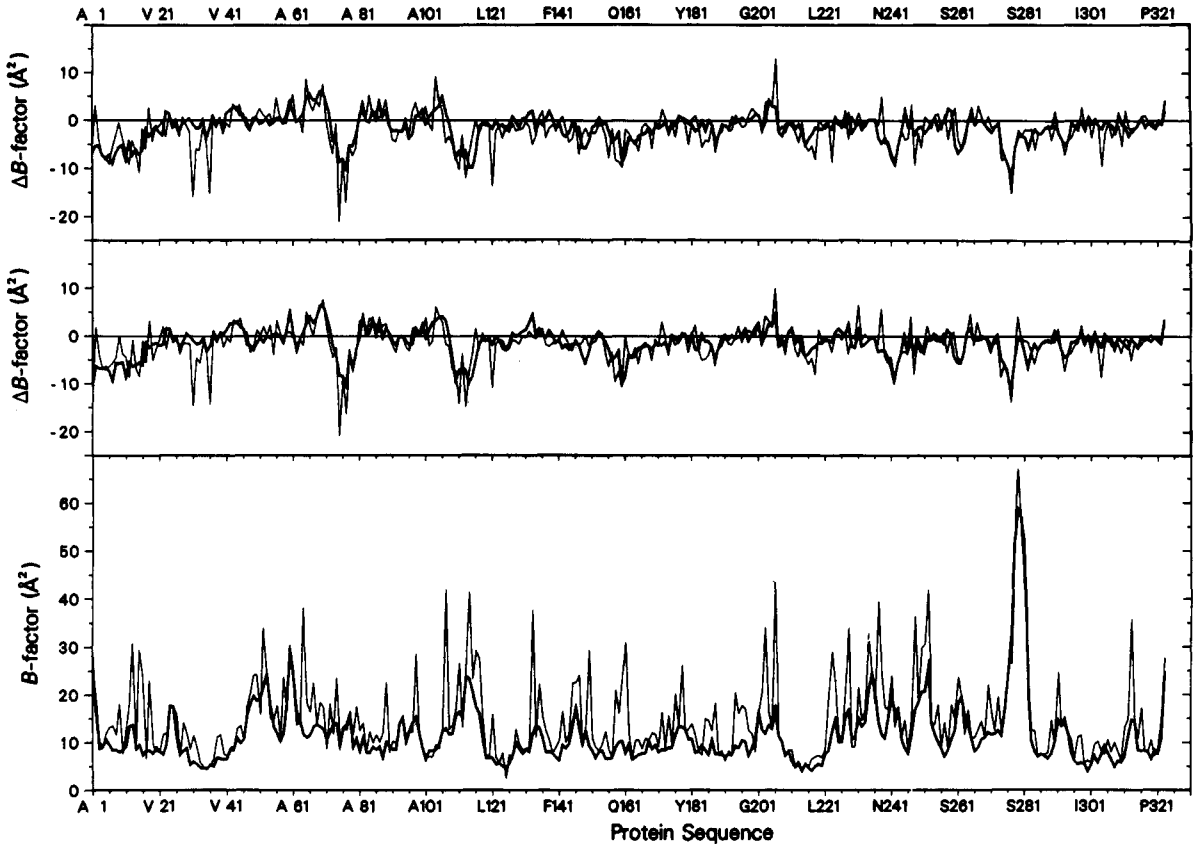

FIGURE 4: Variation of the temperature factor B along the polypeptide chain of the penicillopepsin molecule. In all three panels, the thick lines represent average B values ($\bar{B}$) over the main-chain atoms (N, C^{α}, C, O); the thin lines correspond to the averaged values over the side-chain atoms. Side-chain averages were set to the main-chain values for glycine residues. (a, bottom) The $\bar{B}$ values for the penicillopepsin molecule in the difluorostatone complex. The distribution is almost identical for the difluorostatine complex and very similar to the one refined for the native structure (James & Sielecki, 1983). (b, middle) Differences between the temperature factors of the penicillopepsin molecule in the difluorostatone complex and in the inhibitor-free protein (James & Sielecki, 1983). (c, top) Same as in panel b but for the difluorostatine complex.

Phe295 (289–295 in the $StaF_2$ complex only). Perusal of this list and of the variation of the mean temperature factors along the polypeptide depicted in Figure 4 corroborate that these residues are mostly associated with regions that are less ordered (more mobile) in each of the structures. Those segments of polypeptide chain in the immediate vicinity of the two inhibitors other than the flap exhibit only very small differences in conformation as a result of inhibitor binding.

As already observed for the refined structures of the pepstatin analogue complexes (James & Sielecki, 1987), the binding of the $StaF_2/StoF_2$ inhibitors to the active site of penicillopepsin brings about a reduced conformational flexibility as measured by the lowered average temperature factors ($\bar{B}$, Figure 4). In the native enzyme, the temperature factors of those amino acids that line the substrate binding cleft vary from 4 to 10 Å^2 for the well-ordered regions (i.e., in the vicinity of Asp33 and Asp213) and from 24 to 48 Å^2 in the more conformationally labile regions [i.e., in the flap, residues 72–82, and in the neighboring helical region 108–118 that forms part of the S_1/S_3[2] binding pockets (James & Sielecki, 1983)]. For both $StoF_2/StaF_2$ complexes, the average B factors of even the well-ordered regions (Phe32–Ser36 and Ala212–Thr217) are reduced from those values in the uncomplexed native enzyme by up to −3 Å^2 (for the main-chain atoms of Gly35 and Gly215 the reductions are −3.9 and −5.4 Å^2, respectively). For these same well-ordered regions, some residues have very large reductions in the mean $\bar{B}$ of the side chains, i.e., Asn31, −16.1 Å^2, and Ser36, −15.7 Å^2 (Figure 4b,c). This effect is even more dramatic for the more conformationally flexible parts of the binding cleft. For the atoms of the flap region, the largest changes are associated with the segment from Tyr75 to Asp77. The atoms of the side chains of Tyr75 and Asp77 experience reduced $\bar{B}$ of −21 and −16 Å^2, respectively (Figure 4b,c). In a similar fashion, both inhibitors upon binding reduce the mean $\bar{B}$ factors of the side chains of Leu121 (∼−13 Å^2) and of Ile293 (∼−7 Å^2). All of these residues make important intermolecular contacts to the P_1 and P_1' residues of the inhibitors (Figure 5). Similar decreases in average B factors on inhibitor binding to other aspartic proteinases have been reported (Davies, 1990).

Figure 4b,c shows a marked drop in $\bar{B}$ for residues in the small helical segment from Ile108 to Asn118. The largest reductions are for the atoms of the side chains of Gln111, Gln113, and Gln114. These residues are on the external face of the helix, not in direct van der Waals contact with the atoms of the inhibitor (distances >4.0 Å) but in the vicinity of the flap. It would appear that the reduced thermal motion parameters for this helical segment are due to the better ordering in the complex of the whole region, the flap in particular.

The increased rigidity of the complexes implied by the reduced $\bar{B}$ factors upon binding of inhibitors or substrate alalogues is directly related to a reduction in conformational entropy. As such, it is an unfavorable contribution to the free energy of binding, in the same way that there is an unfavorable reduction in conformational entropy occurring when the free

[2] The nomenclature of Schechter and Berger (1967) is used to describe the interactions of enzyme and inhibitors. P_n and P_n' denote residues on either side of the scissile bond, by definition between P_1 and P_1'. S_n and S_n' denote the corresponding binding pockets in the enzyme.

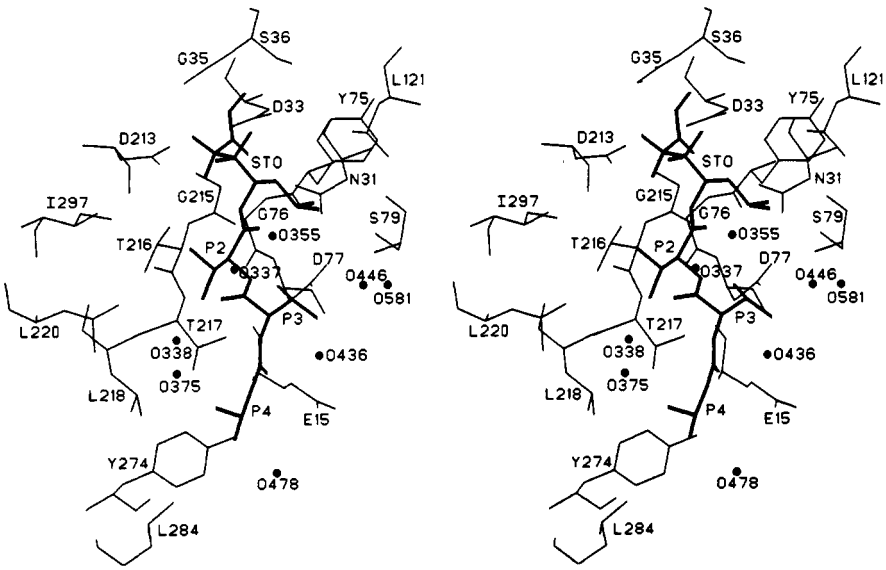

FIGURE 5: Binding of the difluorostatone inhibitor (thick lines) in the active cleft of penicillopepsin. Solvents (filled circles) and residues of the enzyme (thin lines) within a 4.2-Å van der Waals radius from the inhibitors have been included.

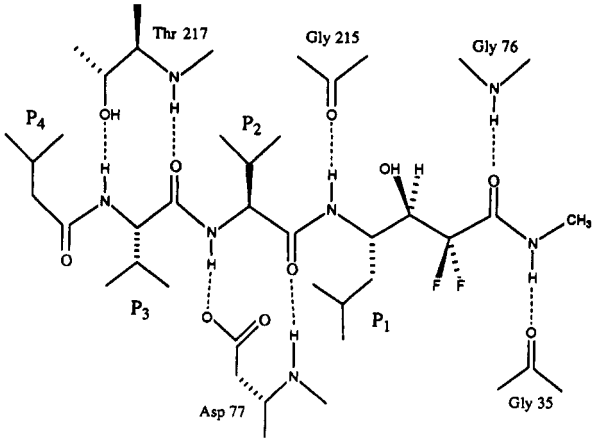

FIGURE 6: Schematics of the hydrogen bonding to the main chain of the inhibitors.

peptide inhibitor binds to the surface of the enzyme. The inability to simulate such behavior reliably and accurately in computers makes the calculation of binding free energies of inhibitors to enzymes extremely difficult, if not impossible, at present.

Hydrogen-Bonding Interactions in the Active Site of Penicillopepsin

(i) Hydrogen Bonds Involving Main-Chain Atoms of the Inhibitors. The carbonyl oxygen atom of the P_4 isovaleryl group points away from the surface of penicillopepsin. It is involved in a hydrogen-bonded interaction with an ordered solvent molecule O436 (Figure 5). The P_3 Val NH forms a hydrogen bond to the side chain $O^{\gamma 1}$ atom of Thr217 in penicillopepsin (Figure 6 and Table V). The carbonyl oxygen atom of P_3 Val receives a hydrogen bond from the main-chain nitrogen of Thr217. The equivalent residue to Thr217 of penicillopepsin is either a threonine or a serine in the vast majority of aspartic proteinases that have been sequenced (Foltmann, 1988; Blundell et al., 1990). Thus, the main-chain hydrogen bonding involving the P_3 residues of substrates or inhibitors is likely to be common among all members of the family of aspartic proteinases. It has been demonstrated in numerous kinetic studies that the residue in the P_3 position has a major effect on k_{cat}/K_m for many substrates in the hydrolytic reaction (Fruton, 1976; Hofmann et al., 1988).

Table V: Contact Distances[a] for Possible Hydrogen Bonding for the $StaF_2$ and $StoF_2$ Inhibitors and Penicillopepsin

	contact atoms			distances (Å)	
	inhibitor		penicillopepsin	$StaF_2$	$StoF_2$
P_3	Val NH	···	Thr217 $O^{\gamma 1}$	2.84	2.89
	Val CO	···	Thr217 NH	2.99	2.97
P_2	Val NH	···	Asp77 $O^{\delta 1}$	3.03	3.03
	Val CO	···	Asp77 NH	3.06	3.08
		···	Gly76 NH	(3.32	3.32)[a]
P_1	Sta(o) NH	···	Gly215 CO	3.18	3.24
	Sta(o) OH1	···	Asp33 $O^{\delta 1}$	(3.49	3.59)[a]
			Asp33 $O^{\delta 2}$	2.65	2.67
			Asp213 $O^{\delta 1}$	2.91	2.91
			Asp213 $O^{\delta 2}$	2.61	2.63
	Sto OH_2	···	Asp33 $O^{\delta 1}$		2.62
			Asp33 $O^{\delta 2}$		(3.29)[a]
P_1'	Me amide NH	···	Gly35 CO	2.88	2.92
	CO	···	Gly76 NH	2.88	2.83

[a] The distances listed in this table conform to the definition of hydrogen-bonding interactions given by Baker and Hubbard (1984). For those distances enclosed within parentheses, the hydrogen-bond donor atom is involved with another acceptor atom for which the distance is 0.5–0.8 Å shorter. The longer distances are associated with weak hydrogen-bonding interactions and have been included here mainly for the sake of completeness.

The flap plays a key role in providing hydrogen-bonding interactions to the residue in the P_2 position (Figure 6 and Table V). As mentioned above, the flap is a very flexible β-hairpin that changes from its open conformation in the native enzyme to a closed conformation in the inhibited form of penicillopepsin (James et al., 1982, 1983). In the inhibitors reported here, the P_2 Val NH forms a hydrogen bond to the side-chain carboxylate of Asp77 $O^{\delta 1}$. A similar interaction can be formed from a model substrate P_2 NH to Thr77 $O^{\gamma 1}$ in porcine pepsin (Sielecki et al., 1990) and human renin (Sielecki et al., 1989). The P_2 Val CO receives hydrogen bonds from the main-chain amide NH of Asp77 (Figure 6 and Table V). The long contact distance Gly76 NH to P_2 Val CO has been included in Table V, but it should probably not be classified as a hydrogen bond because the N–H···O angle deviates markedly from 180° (Figure 5).

The *N*-methyl amide groups present in the $StaF_2$ and $StoF_2$ inhibitors form a hydrogen bond from their amide NH atom to the carbonyl oxygen atom of Gly35 (Figures 6 and 7, Table V). This hydrogen-bonded interaction is not possible with the ethyl ester group on the two inhibitors of penicillopepsin

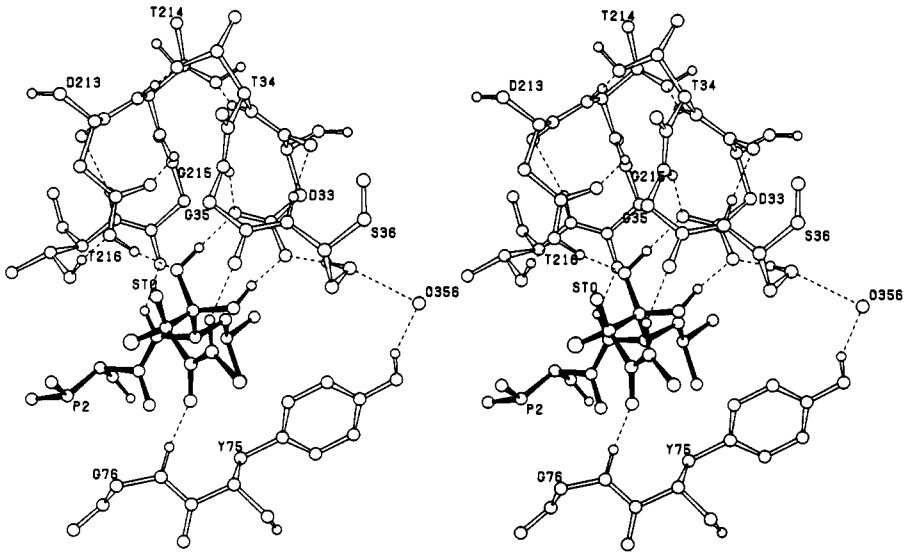

FIGURE 7: Hydrogen-bonding interactions in the active site of penicillopepsin involving the catalytic aspartic acid residues Asp33 and Asp213 and the residue of the difluorostatone inhibitor at the P_1 position. Protons in the active site are positioned according to the scheme depicted in Figure 8c.

studied previously (James et al., 1982, 1985). As a result, the esters are poorly ordered and adopt high-energy nonplanar conformations in order to avoid close contacts with Gly35 (James et al., 1983). The carbonyl oxygen atom of the methyl amide forms a hydrogen bond to the NH of Gly76 on the penicillopepsin flap (Figure 6 and 7). This feature is common to many of the other inhibitors bound to members of the aspartic proteinase family (James et al., 1982, 1983; Suguna et al., 1987; Cooper et al., 1987, 1989; Foundling et al., 1987; Sali et al., 1989). For those inhibitors that span the P_1' and P_2' sites, the Gly76 NH hydrogen bond is to the CO of the P_1' residue, and the NH of the P_2' residue forms the hydrogen bond to the CO of Gly35. An analogous hydrogen bond from the P_2' NH to the carbonyl oxygen atom of residue 41 in the serine proteinases emphasizes the similar substrate-binding mode in these two proteolytic enzyme families (James & Sielecki, 1985).

(ii) Hydrogen-Bonding Interactions in the $StaF_2$ and $StoF_2$ Residues. The NH protons of the $StaF_2$ and the $StoF_2$ moieties form hydrogen bonds to the carbonyl oxygen atom of Gly215 (Figures 6 and 7, Table V). Peptide product inhibitors and protein inhibitors bound to serine proteinases exhibit relatively long contact distances (~3.6 Å) from the NH of the P_1 residues to the carbonyl oxygen atom of Ser214 (or Ser125 in the case of subtilisin) (James et al., 1980; Fujinaga et al., 1982; 1987; Read et al., 1983; Read & James, 1986; McPhalen & James, 1988; Huber & Bode, 1978). In all of these cases, the inhibitors are mimics of the enzyme–substrate complex in which the scissile peptide is not significantly distorted from planarity. It has been proposed that as the substrate carbonyl approaches the tetrahedral transition state, the P_1 NH to Ser214 O hydrogen bond would shorten and strengthen, thereby stabilizing the transition state (Robertus et al., 1972). Short hydrogen bonds have been observed from the NH of P_1 residues of inhibitors that have tetrahedral carbon atoms covalently linked to the active site Ser195 of the serine proteinases (James et al., 1980), thereby supporting this proposal. The statine-based inhibitors have tetrahedral carbon atoms as mimics of the transition state in the aspartic proteinase mechanism. The hydrogen bonds for the P_1 NH groups, however, are ~3.2 Å (Table V). The two carbonyl oxygen atoms of Gly35 and Gly215 are clearly important in providing the correct hydrogen-bonding environment for the P_2' and P_1 residues, respectively, so that the scissile peptide between the P_1 and P_1' residues can be hydrolyzed effectively.

The hydrogen-bonding interactions that involve the inhibitors and the active site carboxyl groups of Asp33 and Asp213 are detailed in Table V and in Figure 7. Since these regions have low *B* factors (Figure 4) and are well defined in the electron density maps, the distances and angles between donor and acceptor atoms that characterize the hydrogen bonds are also well defined. On the other hand, the protonation states of the catalytic aspartates cannot be unambiguously assigned. Each of the carboxyl groups of Asp33 and Asp213 receive two hydrogen bonds from groups with very high proton affinities and for which the protons can be positioned unambiguously. The peptide amides of Gly35 and Gly215 each are a hydrogen-bond donor to the "inner" oxygen atoms, $O^{\delta 2}$ and $O^{\delta 1}$ of Asp33 and Asp213, respectively (Figures 7 and 8). Likewise, the hydroxyl groups of Ser36 and Thr216 each donate protons to the "outer" oxygen atoms, $O^{\delta 1}$ and $O^{\delta 2}$ of Asp33 and Asp213, respectively. The directional character and distances (Figures 7 and 8) of these four hydrogen bonds (N–H···O and O–H···O) fit well with expected stereochemistries for amide and hydroxyl hydrogen-bond donating groups (Baker & Hubbard, 1984).

None of the four hydrogen-bond donor atoms are coplanar with the carboxyl groups with which they are interacting (Figure 7). They are all (Gly35 N, Gly215 N, Ser36 O^{γ}, and Thr216 $O^{\gamma 1}$) approximately 1 Å distant from the respective carboxyl planes. Gly35 N and Ser36 O^{γ} are both on the same side of the plane of the carboxyl group of Asp33. Similarly, Gly215 N and Thr216 $O^{\gamma 1}$ are on the same side of the plane of the carboxyl group of Asp213. Figure 7 also shows that these four hydrogen bonds are all donated toward the anti lone pair electrons on the oxygen atoms. This leaves the syn lone pair electrons on the active site carboxyl group oxygen atoms free to be involved with the proton transfers that must take place during a catalytic cycle (Gandour, 1981). Whether or not the syn lone pair orbitals are more basic than the anti lone pairs is quite controversial at present (Allen & Kirby, 1991). What is remarkable, however, is that in proteins the syn lone pair orbitals of the carboxylate groups of aspartate and glutamate residues seem to be favored in a functional role of proton transfer in hydrolase enzymes. This may be a steric requirement rather than one of enhanced basicity.

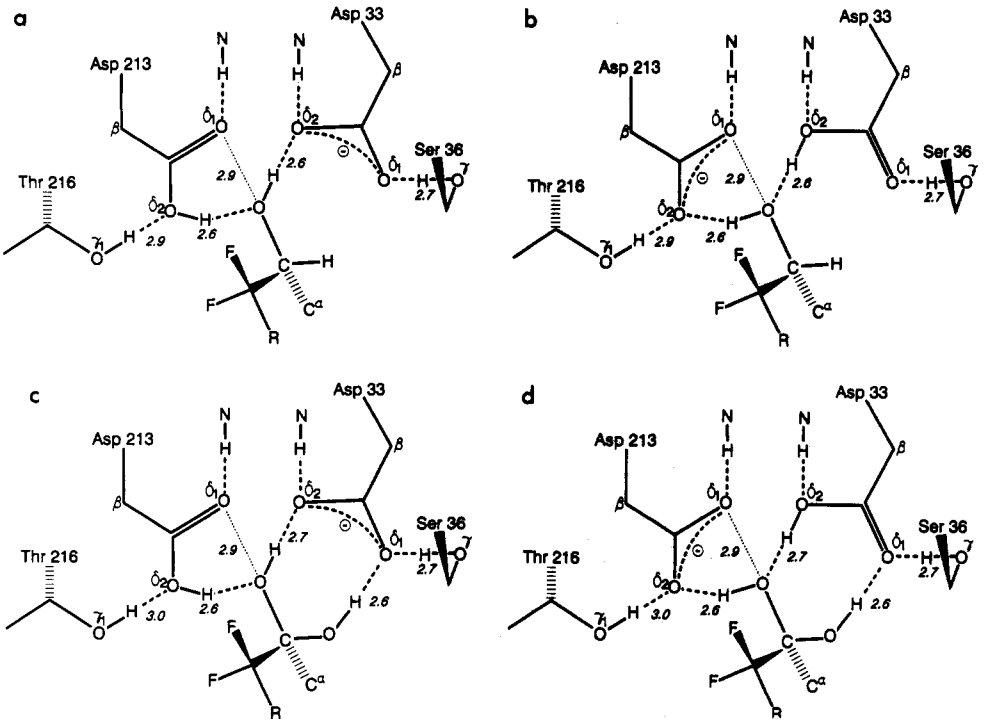

FIGURE 8: Possible hydrogen-bonding scheme alternatives proposed for the active site of penicillopepsin with bound difluorostatine (a and b) or difluorostatone (c and d) inhibitors.

On the basis of the observed hydrogen bond and interatomic contact distances involving the oxygen atoms of the catalytic carboxyl groups and the $StaF_2$ and $StoF_2$ groups of the two statine inhibitors, we propose two likely proton position scenarios (Figure 8a–d). In each of these cases, the active site region has a net negative charge. This charge is most likely dissipated by the positive ends of the dipole moments of the hydrogen bonds directed toward the carboxyl groups. At the present resolution of our crystallographic structures, it is not possible to determine experimentally the positions of the protons. Therefore, comparison of Figure 8, panels a and b, for the difluorostatine residue indicates that from our data it is not possible to differentiate whether the negative charge is on Asp33 or on Asp213.

As shown in Figure 8a, the proton on the (*R*)-3-hydroxyl group of $StaF_2$ forms a hydrogen bond (2.6 Å) to the negatively charged carboxylate of Asp33. Asp213 is shown protonated on $O^{\delta 2}$ because the distance from Asp213 $O^{\delta 2}$ to the (*R*)-3-OH group (2.6 Å) is ~0.3 Å shorter than that from the Asp213 $O^{\delta 1}$ to the (*R*)-3-OH group (2.9 Å). This difference of 0.3 Å is barely statistically significant based on a coordinate accuracy of ~0.12 Å for the most well ordered part of the structure (*B* factors <10 $Å^2$). However, in all of the independently determined statine-based inhibitor complexes with penicillopepsin, this difference is consistently observed to be in the same direction and of similar magnitude. Thus, the distances Asp213 $O^{\delta 1}$···(*R*)-3-OH (2.9 Å) and Asp213 $O^{\delta 1}$···Asp33 $O^{\delta 2}$ (3.1 Å) are taken as normal van der Waals contacts between these three atoms. On the other hand, Figure 8b shows the disposition of protons in the active site region that would place the negative charge on the carboxylate group of Asp213. It is not possible to distinguish between these two hydrogen-bonding schemes on the basis of the contact distances alone. As proposed for the scheme detailed in Figure 8a, Asp213 $O^{\delta 1}$ makes normal van der Waals contacts and not hydrogen-bonded interactions with Asp33 $O^{\delta 2}$ and the (*R*)-3-OH group. The atomic positions in $StaF_2$ relative to the two carboxyl groups make it unlikely that the active site is neutral. Attempts to place a proton on either carboxylate group in a stereochemically acceptable position results in too close contacts with other protons.

The hydrogen-bonding schemes proposed for the $StoF_2$ inhibitor are shown in Figure 8, panels c and d. Both schemes portray the hydrated $StoF_2$ as a *gem*-diol. In Figure 8c the two hydroxyl groups are shown donating protons to the two oxygen atoms of the negatively charged carboxylate of Asp33. These two hydrogen-bonded distances are of approximately equal length (2.6 Å) and are similar to the hydrogen-bond length of the $StaF_2$ (*R*)-3-OH to Asp33 $O^{\delta 2}$ (Figure 8a). The carboxyl group of Asp213 is protonated, and the distance from Asp213 $O^{\delta 2}$ to the hydroxyl group has the same value as the equivalent distance in the $StaF_2$ inhibitor complex (2.6 Å). Figure 8d depicts the alternative hydrogen-bonding scheme when the net negative charge is localized on the carboxylate of Asp213. Both of the schemes shown in Figure 8, panels c and d are equally probable on a steric basis and suggest that this resonance stabilization could be an important feature of the aspartic proteinase active site.

It is possible that a fourth proton could be added to the active site of the $StoF_2$-containing inhibitor that would preserve the hydrogen-bonding stereochemistry but would result in a neutral active site. Rotation of the proton on the "outer" oxygen of $StoF_2$ by ~120° (Figure 8c) to an alternative staggered conformation would allow protonation of Asp33 $O^{\delta 1}$. The hydrogen-bonding interaction would be preserved by this protonation, but the net negative charge on the active site would be neutralized. It may be possible to detect this alternative experimentally by analyzing the pH behavior of K_i for $StoF_2$-containing peptides. Because the hydrogen-bonding distances are so similar among the statine-based inhibitors, this latter alternative for $StoF_2$ is probably not realized with the present conditions of pH 4.4 and high salt concentration.

As mentioned above, replacement of the outer hydroxyl group of the $StoF_2$-containing inhibitor with a hydrogen results in a 10-fold increase in the K_i. This decrease in binding free energy of 1.4 kcal/mol is typical for the loss of a single non-

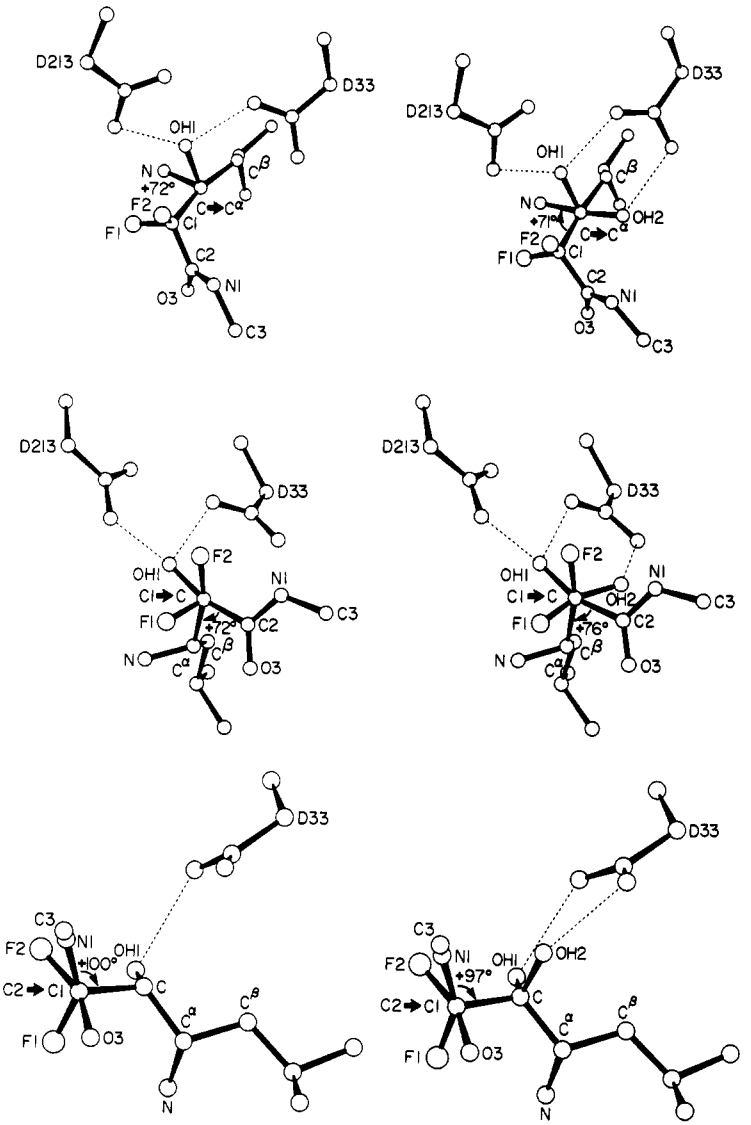

FIGURE 9: Conformational diagrams for the $StaF_2/StoF_2$ groups of the difluorostatine and difluorostatone inhibitors bound to penicillopepsin.

ionic hydrogen bond (Street et al., 1986; Fersht et al., 1985). If the outer hydroxyl group interacts with a negatively charged acceptor on the enzyme, the loss of this potential hydrogen bond to an ionic group might be expected to cause a more substantial decrease in the binding free energy (typically greater than 3 kcal/mol) (Street et al., 1986; Fersht et al., 1985). Although this suggests a preference for the hydrogen-bonding scheme shown in Figure 8d over the one shown in Figure 8c, it is premature to rule out one of these only on the basis of relative inhibitor energies. In addition, it is difficult to calculate the relative affinities of the $StaF_2$- vs $StoF_2$-containing inhibitors using free energy perturbation methods without a precise knowledge of the hydrogen positions in the enzyme's active site. Further studies using either neutron diffraction or ^1H and ^{13}C NMR would be necessary to resolve this ambiguity.

The Conformations of $StaF_2$ and Hydrated $StoF_2$

The least-squares comparison of the atomic coordinates of the two inhibitors described in a previous section shows how similar the two structures are. Analysis of the conformational diagrams shown in Figure 9 and the main-chain conformational angles listed in Table VI confirms the remarkable similarity in the mode of binding of these two molecules. Table VI also shows that the other two statine-based inhibitors in association with penicillopepsin that have been previously studied crystallographically also adopt conformations that are, within the limits of accuracy of the determinations, identical to that of the two $StaF_2/StoF_2$ inhibitors.

The conformational angle (N–C^α–C–C1) at the P_1 $StaF_2/StoF_2$ residue that is analogous to the ψ angle in a peptide is in the region of +70° (Figure 9a). This is approximately 50° from the value associated with an extended β-strand ($\phi = -130$, $\psi = +120$). Nonetheless, even with this angle the chain still has a partially extended conformation. The next angle (C^α–C–C1–C2, analogous to the peptide bond ω angle) is very far from the trans (antiperiplanar) conformation of 180° (Figure 9b). The corresponding atoms are all approximately in the positions of a staggered conformation that is opened up by approximately 15° (to +75°). There are two likely steric reasons for this marked departure from the trans conformation. If this angle were close to 180°, then steric clashes of the two fluorine atoms could occur with the atoms of the preceding peptide bond. The main determinant for the observed conformation, however, seems to be the favorable hydrogen-bonding interactions of the *N*-methyl amide (Figures 6 and 7; Table V). As described above, this group donates a hydrogen bond to Gly35 O and is the recipient of a hydrogen bond from Gly76 NH.

The third conformational angle (C–C1–C2–N) corresponds to an orthonormal orientation (~90°). It is probably the most

Table VI: Conformational Angles (deg) of Statine-Based Inhibitors Bound to Penicillopepsin

	IvaVV-StaOEt	IvaVV-LystaOEt	IvaVV-Sta-F_2NHCH_3	IvaVV-Sto-F_2NHCH_3
P_4 Iva				
ψ^a	−120	−164	−160	−160
ω	−174	−179	−178	−177
$\chi^{1\,a}$	−46	57	62	61
P_3 Val				
ϕ	−116	−108	−111	−110
ψ	163	166	168	166
ω	175	178	179	−179
χ^1	−69	−61	−56	−57
P_2 Val				
ϕ	−130	−134	−134	−138
ψ	97	99	99	101
ω	−179	−179	−178	−178
χ^1	−173	−176	−173	−175
P_1 Sta				
ϕ	−116	−124	−124	−124
ψ^a	52	60	73	71
ω^a	118	103	72	76
χ^1	−55	−51	−53	−53
χ^2	171	−57	174	176
χ^3		−173		
χ^4		−160		
C–C1–C2–N (O4)	110	139	100	97
A	−87		180	180

[a] For the Iva group the ψ angle is defined as CB–CA–C–N(P3), and the χ^1 is defined as CG1–CB–CA–C. The main-chain conformational angles for the statine groups are defined as ψ (N–CA–C–C1) and ω (CA–C–C1–C2). The atom nomenclature for these groups is shown below:

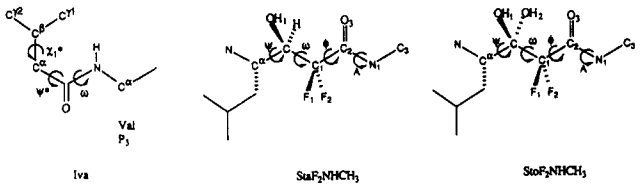

stable conformation for this group, but our failure to locate an equivalent small molecule structure in the Cambridge Crystallographic Database makes it impossible to state this unambiguously. This orthonormal conformation is also stabilized by the hydrogen-bonding interactions of the amide discussed above (Figure 6 and 7).

Implications for Catalysis by Aspartic Proteinases

The currently held views regarding a catalytic mechanism for the aspartic proteinases have been summarized in a number of review articles (Hofmann et al., 1984; James & Sielecki, 1987; Davies, 1990). Following the original suggestions of Fruton (1976), all authors of the mechanisms based on structural results have agreed that the catalytic pathway does not involve covalently attached acyl or amino intermediates, rather, that the hydrolysis proceeds via a noncovalently bound tetrahedral intermediate arising from a general base-assisted attack of a water molecule on the carbonyl carbon of the scissile peptide. It is the identification of the nucleophilic water molecule that has been controversial (James & Sielecki, 1985, 1987; Davies, 1990; Pearl & Blundell, 1984). James and Sielecki (1985) have proposed that the attacking nucleophile is a water molecule bound to the "outer" oxygen atom ($O^{\delta 1}$) of Asp33. The other authors assign this role to the central water molecule that binds to the active site carboxyl groups in a remarkably conserved position in all aspartic proteinases of known structure (Figure 10a). The hydrogen-bonding interactions that we have deduced from the present analysis of the $StaF_2$- and $StoF_2$-containing inhibitors bound to penicillopepsin have prompted a reevaluation of our proposed catalytic pathway for the hydrolysis of peptides by the aspartic proteinases. The results are summarized in Figure 10a–e in which the role of the nucleophile is ascribed to the central water molecule and the overall mechanism is similar to that proposed by Suguna et al. (1987).

There are many alternative hydrogen-bonding patterns that one can propose for the native aspartic proteinase enzymes [see, for example, James and Sielecki (1987)]. These schemes must be consistent with the pH of the solution, the stereochemistry of hydrogen bonding (Baker & Hubbard, 1984), and the pK_a values for the system of two hydrogen-bonded carboxylate groups (Asp33 and Asp213 in the case of penicillopepsin). The difficulty in interpreting the experimental results is compounded by the uncertainty about which carboxyl group carries the negative charge at pH values near the optimum of catalytic activity (2–4). Also, there is uncertainty in whether or not the carboxyl groups of Asp33 and Asp213 ever share a proton in a hydrogen-bonded interaction. Analogy with the maleic acid–maleate monoanion has been made for these carboxyl groups (James & Sielecki, 1983, 1985, 1987). However, the only evidence that Asp33 and Asp213 share a hydrogen-bonded proton (between Asp33 $O^{\delta 2}$ and Asp213 $O^{\delta 1}$) in the native enzyme is the $O^{\delta 2}\cdots O^{\delta 1}$ distance of 2.9 Å observed for most aspartic proteinases of known structure. On the other hand, this is a perfectly reasonable O···O nonbonded contact distance since oxygen atoms have a van der Waals radius of 1.4 Å. Thus, the proton may indeed by resident on one of the other two oxygen atoms of these carboxyl groups (Suguna et al., 1987).

The chemical identity associated with the electron density peak always found within hydrogen-bonding distance of the two carboxyl groups in the native enzymes is also ambiguous (James & Sielecki, 1983, 1985, 1987; Davies, 1990). The magnitude of the peak and integration of the number of electrons associated with it makes it consistent with that expected for a water molecule. However, the fact that there will be a net negative charge in the active site at the pH optima of these enzymes (Knowles, 1970) and that this solvent site is also a site for the binding of positively charged ions in aspartic proteinases [e.g., Tl^+ and UO_2^+ for penicillopepsin (James & Sielecki, 1985)] was taken as strong evidence that it could be occupied by a positively charged counterion. There are several alternatives which are isoelectronic and of similar van der Waals or ionic radius to a water molecule, and in previous publications of the Edmonton laboratory (James & Sielecki, 1983, 1985) it was speculated that it could correspond to an ammonium ion (NH_4^+), an oxonium ion (H_3O^+), or a sodium ion (Na^+). The least likely of these alternatives is the sodium ion because Na^+ ions prefer an octahedral coordination of six oxygen ligands at distances of 2.4 Å. The disposition of the two carboxyl groups in the active sites of the aspartic proteinases precludes octahedral coordination. The presence of a similar peak isostructurally positioned in rhizopuspepsin, which was crystallized at pH 6 in the absence of ammonium ions, weakens the proposal of an NH_4^+ ion (Suguna et al., 1987). All of the evidence is, unfortunately, circumstantial. Therefore, we represent a likely scenario for the hydrogen bonding in the active site of native penicillopepsin in which the electron density peak between the two carboxyl groups has been interpreted as a water molecule (Figure 10A). This is probably the concensus among the many papers written on this subject. Also, in agreement with the proposals of Suguna et al. (1987), Figure 10A shows that the net negative charge in the active site is resident on the carboxylate of Asp213 with

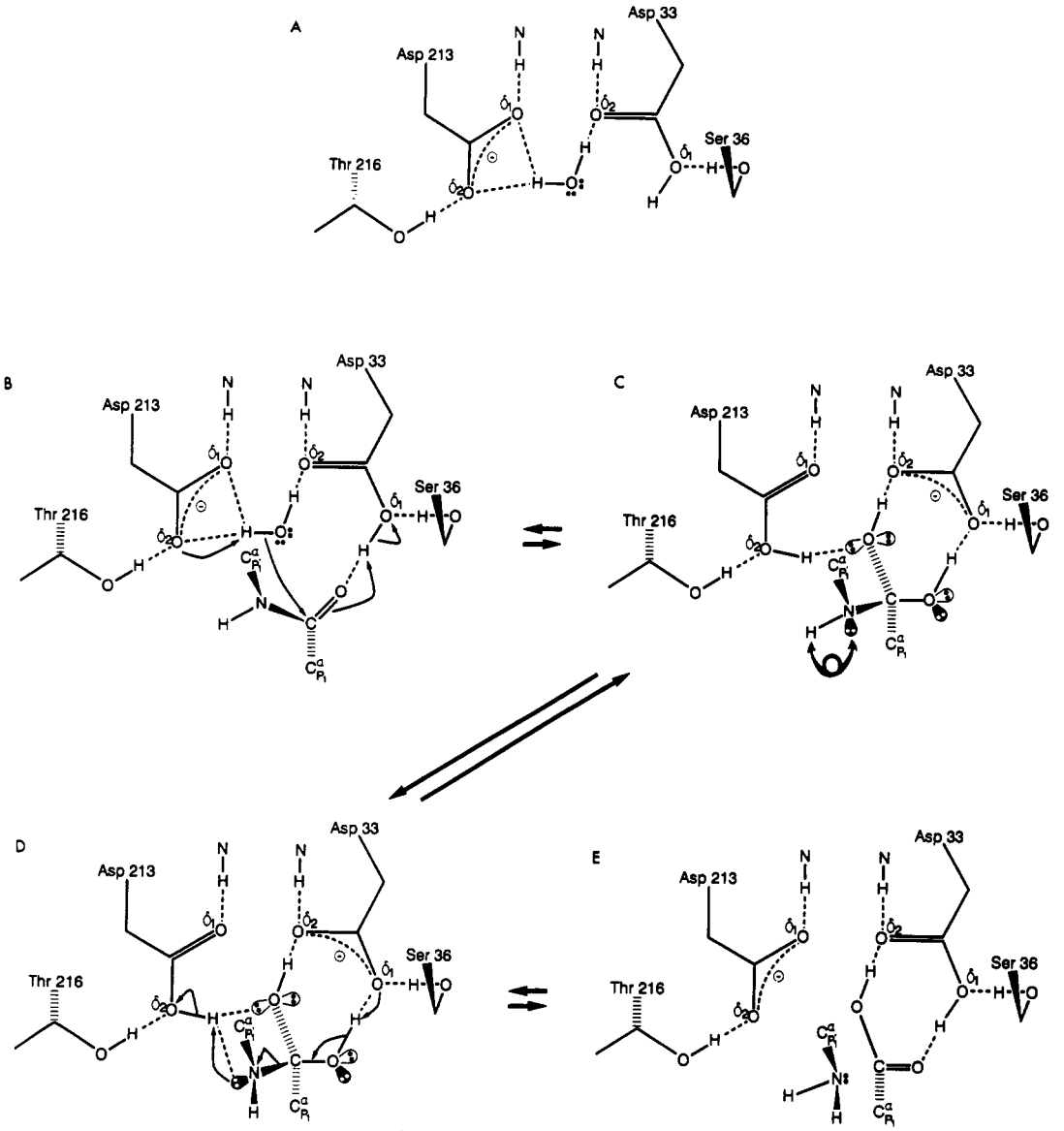

FIGURE 10: Proposed scheme for the catalytic pathway of peptide hydrolysis by aspartic proteinases. (A) A possible hydrogen-bonding scheme in the active site of native uncomplexed penicillopepsin. The water molecule shown between the two aspartic acid residues is the nucleophilic group. Asp213 has the role of a general base; Asp33 is the general acid. (B) The approach of a scissile peptide of a substrate to the active site of penicillopepsin. The orientation of this peptide is based on molecular modeling described by James and Sielecki (1985). The electrophilic centre that would enhance the polarization of the carbonyl bond of the substrate is the hydrogen bond from the carboxyl group of Asp33 and the partial positive charge on the edge of the phenolic ring of Tyr75 (not shown). The movement of electrons in this concerted nucleophilic attack is indicated by the thin arrows. (C) The proposed noncovalently bound tetrahedral intermediate on the catalytic pathway. Both the carbonyl carbon atom and the nitrogen atom of the scissile peptide are shown as tetrahedral sp^3 atoms. Stabilization of this tetrahedral intermediate is achieved by a hydrogen-bonding scheme for the *gem*-diol that is identical to that deduced for the $StoF_2$ mimic as shown in Figure 8c. Lone pair electron orbitals on the heteroatoms (N and O) of the tetrahedral intermediate are shown. The formation of the tetrahedral intermediate by the nucleophilic attack of the water molecule is assisted by the lone pair electron orbitals oriented *antiperiplanar* to the direction of attack (the orbitals on the nitrogen and the carbonyl oxygen atoms that are shaded). Inversion of configuration of the nitrogen atom of the tetrahedral intermediate, required for the protonation by Asp213, is indicated by the curly arrows. (D) The breakdown of the tetrahedral intermediate is represented by the concerted movement of electron pairs (thin arrows) from Asp33 to Asp213 in a manner that is the reverse of the formation of the tetrahedral intermediate (panel B). The proton that is transferred to the nitrogen atom from Asp213 in order to make the nitrogen a good leaving group (i.e., R-NH_2) originated on the nucleophilic water in this scheme. Cleavage of the C–N bond receives stereoelectronic assistance from the *antiperiplanar* orientation of the lone pair electron orbitals on the two oxygen atoms of the tetrahedral intermediate (unshaded in this figure). (E) The peptide bond is hydrolyzed. The products will diffuse from the enzyme surface to be replaced by a water molecule, thus regenerating the active site of penicillopepsin as shown in panel A.

the carboxyl group of Asp33 $O^{\delta 1}$ protonated and neutral. The water molecule is shown forming a hydrogen bond to Asp33 $O^{\delta 2}$ at a distance of 2.6 Å. This distance is in the range 2.6–2.9 Å in all the members of the aspartyl proteinase family. The distance from the water to Asp33 $O^{\delta 1}$ is consistently longer in all of the native enzymes and generally too long to be considered a strong hydrogen bond. The second proton on the water molecule is shown making a bifurcated hydrogen bond to both oxygen atoms of the Asp213 carboxylate. This is consistent with the observation that both distances are of approximately equal length (2.8–2.9 Å on average).

In Figure 10A–E as in the separate panels of Figure 8, the hydrogen bonding from the residues in the immediate environment of the two carboxyl groups (Gly35 NH, Gly215 NH, Ser36 $O^{\gamma}H$, and Thr216 $O^{\gamma 1}H$) is shown unchanged from panel to panel. However, minor alterations in the conformation of the enzyme could influence the strength of these hydrogen bonds which, in turn, may have a subtle effect on the relative

basicity of the two carboxyl groups during a catalytic cycle. In particular, the relative orientation of the two peptide dipoles, Thr34–Gly35 and Thr214–Gly215, could have a profound electrostatic influence on the distribution of electrons and protons in the active site of penicillopepsin in the presence of substrates. Different conformational changes have been observed in endothiapepsin in the presence of different inhibitors (Sali et al., 1989). Similar effects could almost certainly happen with the other aspartic proteinases (Sielecki et al., 1990).

Nucleophilic attack on the substrate carbonyl carbon atom by the central water molecule is assisted by several factors shown diagrammatically in Figure 10B,C. The nucleophilic character of the central water molecule is augmented by the general base function of the carboxylate of Asp213. Enhanced polarization of the carbonyl bond (i.e., making the carbon atom more positively charged) would result from the relatively electrophilic environment of the carbonyl oxygen atom. It would initially be the recipient of a hydrogen bond from the carboxyl group of Asp33 $O^{\delta 1}H$. Subsequently, Asp33 plays the role of general acid in this scheme. It is likely that the proton affinity of a *gem*-diol would be much greater than that of an aspartyl carboxylate (Figure 10C). The partially positively charged edge of the phenolic ring of Tyr75 would come within 4 Å of the carbonyl oxygen atom, thus additionally enhancing the electrophilic environment (Blundell et al., 1987). Figure 10C also shows the stereoelectronic assistance to the formation of the hydroxyl–carbon bond. There are lone pair electron orbitals on the nitrogen and oxygen atoms of the substrate that can be oriented *antiperiplanar* to the new O–C bond that is being formed. The nitrogen atom of the scissile peptide adopts a tetrahedral character, as does the carbonyl carbon atom, during this step. Thus, the geometry of the groups at the active site conforms well with the stereoelectronic principles (Deslongchamps, 1975) or equally, with the principle of least nuclear motion (Hine, 1977).

Before a proton can be transferred to the nitrogen of the leaving group, it is necessary to invert the configuration of the nitrogen atom (Figure 10C,D). This analogous problem has been discussed in the case of the serine proteinases (Bizzozero & Dutler, 1981). For that enzyme family, it was proposed that the configuration of the groups bonded to the nitrogen atom could be changed by inversion of the nitrogen atom through the plane of the other three substituents. In our case, this would result in the presentation of the lone pair electrons on the nitrogen atom for protonation by Asp213 (Figure 10C,D). The rate of inversion at nitrogen centers is rapid and of the order of 10^9 s^{-1} (Bizzozero & Dutler, 1981).

Many of the features of the catalytic active site of the aspartic proteinases have analogous components in the serine proteinases. The electrophilic oxyanion hole of the serine proteinases has its analogue in the hydrogen bond from Asp33 and the positively charged edge of the phenolic ring of Tyr75. The nucleophilic serine alkoxide ($-CH_2-O^-$) has as its equivalent the centrally bound water molecule. In the serine proteinases the role of the general base is played by the imidazole ring of a histidyl residue. In the aspartic proteinases this role is provided by the carboxylate of Asp213. The similarity in substrate binding by the members of these two enzyme families has been discussed (James & Sielecki, 1985, 1987).

Cleavage of the peptide bond is represented by the breakdown of the tetrahedral intermediate (Figure 10D,E). The two oxygen atoms of the tetrahedral intermediate have lone pair electron orbitals oriented *antiperiplanar* to the C–N bond (Figure 10D). Proton transfer from the carboxyl group of Asp213 to the lone pair electron orbital on the P_1' nitrogen atom would produce the good leaving group (Figure 10D,E). Finally, the diffusion of the products from the active site and replacement of the carboxyl of the leaving group with a water molecule would generate the native enzyme ready for another round of catalysis.

In the previous proposals from this laboratory, the attacking nucleophile originated from a water molecule that was hydrogen bonded exclusively to Asp33. Our present analysis makes it more likely that this water molecule is displaced on substrate binding. It was also deemed that the negatively charged carboxylate at the active pH was that from Asp33. With the data now available based on the binding interactions of the $StaF_2$ and $StoF_2$ inhibitors, it would seem that the interpretations depicted in Figure 10 correspond to the more likely mechanism for the aspartic proteinases, substantially in agreement with earlier proposals (Suguna et al., 1987).

ACKNOWLEDGMENTS

We thank Theo Hofmann for the sample of the colorimetric substrate and Dan Rich for the sample of IvaValValStaOEt. Michael Allegretto and Rafe McNab helped in preparation of some of the figures.

REFERENCES

Allen, F. H., & Kirby, A. J. (1991) *J. Am. Chem. Soc. 113*, 8829–8831.

Aoyagi, T., Morishima, H., Nishizawa, R., Kunimoto, S., Takeuchi, T., Umezawa, H., & Ikezawa, H. (1972) *J. Antibiot. 25*, 689–694.

Baker, E. N., & Hubbard, R. E. (1984) *Prog. Biophys. Mol. Biol. 44*, 97–179.

Barry, C. D., Molnar, C. E., & Rosenberger, F. U. (1976) MMS-X molecular modelling system, Washington University, St. Louis, MO.

Bartlett, P. A., & Kezer, W. B. (1984) *J. Am. Chem. Soc. 106*, 4282–4283.

Bernstein, F. C., Koetzle, T. F., Williams, G. J. B., Meyer, E. F., Jr., Brice, M. D., Rodgers, J. R., Kennard, O., Shimanouchi, T., & Tasmui, M. (1977) *J. Mol. Biol. 112*, 535–542.

Bizzozero, S. A., & Dutler, H. (1981) *Bioorg. Chem. 10*, 46–62.

Blundell, T. L., Cooper, J., Foundling, S. I., Jones, D. M., Atrash, B., & Szelke, M. (1987) *Biochemistry 26*, 5585–5590.

Blundell, T. L., Jenkins, J. A., Sewell, B. T., Pearl, L. H., Cooper, J. B., Wood, S. P., & Veerapandian, B. (1990) *J. Mol. Biol. 211*, 919–941.

Cooper, J. B., Foundling, S. I., Hemmings, A. M., Blundell, T. L., Jones, D. M., Hallett, A., & Szelke, M. (1987) *Eur. J. Biochem. 169*, 215–221.

Cooper, J. B., Foundling, S. I., Blundell, T. L., Boger, J., Jupp, R. A., & Kay, J. (1989) *Biochemistry 28*, 8596–8603.

Davies, D. R. (1990) *Annu. Rev. Biophys. Biophys. Chem. 19*, 189–215.

Deslongchamps, P. (1975) *Tetrahedron 31*, 2463–2490.

Fearon, K., Spaltenstein, A., Hopkins, P. B., & Gelb, M. H. (1987) *J. Med. Chem. 30*, 1617–1622.

Fersht, A. R., Shi, J. P., Knill-Jones, J., Lowe, D. M., Wilkinson, A. J., Blow, D. M., Brick, P., Cortes, P., Waye, M. M. Y., & Winter, G. (1985) *Nature (London) 314*, 235–238.

Foltmann, B. (1988) in *Proceedings of the 18th Linderstrom-Lang Conference: Aspartic Proteinases* (Foltmann, B., Ed.) pp 7–20, University of Copenhagen, Copenhagen.

Foundling, S. I., Cooper, J., Watson, F. E., Cleasby, A., Pearl., L. H., Sibanda, B. L., Hemmings, A., Wood, S. P., Blundell, T. L., Valler, M. J., et al. (1987) *Nature (London) 327*, 349–352.

Fruton, J. S. (1976) *Adv. Enzymol. Relat. Areas Mol. Biol. 44*, 1–36.

Fujinaga, M., Read, R. J., Sielecki, A., Ardelt, W., Laskowski, M., Jr., & James, M. N. G. (1982) *Proc. Natl. Acad. Sci. U.S.A. 79*, 4868–4872.

Fujinaga, M., Sielecki, A. R., Read, R. J., Ardelt, W., Laskowski, M., Jr., & James, M. N. G. (1987) *J. Mol. Biol. 195*, 397–418.

Gandour, R. D. (1981) *Bioorg. Chem. 10*, 169–176.

Gelb, M. H., Svaren, J. P., & Abeles, R. H. (1985) *Biochemistry 24*, 1813–1817.

Hendrickson, W. A. (1976) *J. Mol. Biol. 106*, 889–893.

Hendrickson, W. A. (1985) *Methods Enzymol. 115*, 252–270.

Hendrickson, W. A., & Konnert, J. H. (1981) in *Biomolecular Structure, Function, Conformation and Evolution* (Srinivasan, R., Ed.) Vol. 1, pp 43–57, Pergamon, Oxford.

Hine, J. (1977) *Adv. Phys. Org. Chem. 15*, 1–61.

Hofmann, T., & Hodges, R. S. (1982) *Biochem. J. 203*, 603–610.

Hofmann, T., Dunn, B., & Fink, A. L. (1984) *Biochemistry 23*, 5247–5256.

Hofmann, T., Allen, B., Bendiner, M., Blum, M., & Cunningham, A. (1988) *Biochemistry 27*, 1140–1146.

Huber, R., & Bode, W. (1978) *Acc. Chem. Res. 11*, 114–121.

Ikota, N., Shiori, T., Yamada, S., & Tachibana, S. (1980) *Chem. Pharm. Bull. 28*, 3347–3352.

James, M. N. G., Hsu, I.-N., & Delbaere, L. T. J. (1977) *Nature (London) 267*, 808–813.

James, M. N. G., & Sielecki, A. R. (1983) *J. Mol. Biol. 163*, 299–361.

James, M. N. G., & Sielecki, A. R. (1985) *Biochemistry 24*, 3701–3713.

James, M. N. G., Sielecki, A. R., Brayer, G. D., Delbaere, L. T. J., & Bauer, C.-A. (1980) *J. Mol. Biol. 144*, 43–89.

James, M. N. G., Sielecki, A., Salituro, F., Rich, D. H., & Hofmann, T. (1982) *Proc. Natl. Acad. Sci. U.S.A. 79*, 6137–6141.

James, M. N. G., Sielecki, A. R., & Moult, J. (1983) in *Peptides Structure and Function, Proceedings of the VIII American Peptide Symposium* (Hruby, V. J., & Rich, D. H., Eds.) pp 521–530, Pierce Chemical Co., Rockford, IL.

James, M. N. G., Sielecki, A. R., & Hofmann, T. (1985) in *Aspartic Proteinases and Their Inhibitors* (Kostka, V., Ed.) pp 163–177, Walter de Gruyter, Berlin.

James, M. N. G., & Sielecki, A. R. (1987) in *Biological Macromolecules and Assemblies* (Jurnak, F. A., & McPherson, A., Eds.) Vol. 3, pp 413–482, John Wiley and Sons, New York.

James, M. N. G., Sielecki, A. R., Murphy, M. E. P., & Gelb, M. H. (1988) in *Proceedings of the 1988 Miami Bio/Technology Winter Symposium* (Brew, K., et al., Eds.) pp 192–193, IRL Press, Washington, D.C., and Miami, FL.

Knowles, J. R. (1970) *Philos. Trans. R. Soc. London, B257*, 135–146.

Kunimoto, S., Aoyagi, T., Nishizawa, R., Komai, T., Takeuchi, T., & Umezawa, H. (1974) *J. Antibiot. 27*, 413–418.

Marciniszyn, J. J., Hartsuck, J. A., & Tang, J. (1976) *J. Biol. Chem. 251*, 7088–7094.

Marshall, G. R. (1976) *Fed. Proc. 35*, 2494–2501.

McPhalen, C. A., & James, M. N. G. (1988) *Biochemistry 27*, 6582–6598.

Morishima, H., Takita, T., Aoyagi, T., Takeuchi, T., & Umezawa, H. (1970) *J. Antibiot. 23*, 263–265.

Morrison, J. F., & Walsh, C. T. (1988) *Adv. Enzymol. Relat. Areas Mol. Biol. 61*, 201–301.

North, A. C. T., Phillips, D. C., & Mathews, F. S. (1968) *Acta Crystallogr. A24*, 351–359.

Pearl, L., & Blundell, T. (1984) *FEBS Lett. 174*, 96–101.

Read, R. J., & James, M. N. G. (1986) in *Proteinase Inhibitors* (Barrett, A. J., & Salvesen, G., Eds.) Chapter 7, pp 301–336, Elsevier, Amsterdam.

Read, R. J., Fujinaga, M., Sielecki, A. R., & James, M. N. G. (1983) *Biochemistry 22*, 4420–4433.

Rich, D. H. (1985) *J. Med. Chem. 28*, 263–273.

Rich, D. H., Bernatowicz, M. S., & Schmidt, P. G. (1982) *J. Am. Chem. Soc. 104*, 3535–3536.

Rich, D. H., Salituro, F. G., & Holladay, M. W. (1983) in *Peptides, Structure and Function, Proceedings of the VIII American Peptide Symposium* (Hruby, V. J., & Rich, D. H., Eds.) pp 511–520, Pierce Chemical Co., Rockford, IL.

Rich, D. H., Salituro, F. G., Holladay, M. W., & Schmidt, P. G. (1984) in *Conformationally Directed Drug Design* (Vida, J. A., & Gordon, M., Eds.) ACS Symposium Series No. 251, pp 211–237, American Chemical Society, Washington, D.C.

Rich, D. H., Bernatowicz, M. S., Agarwal, N. S., Kawai, M., Salituro, F. G., & Schmidt, P. G. (1985) *Biochemistry 24*, 3165–3173.

Robertus, J. D., Kraut, J., Alden, R. A., & Birktoft, J. J. (1972) *Biochemistry 11*, 4293–4303.

Sali, A., Veerapandian, B., Cooper, J. B., Foundling, S. I., Hoover, D. J., & Blundell, T. L. (1989) *EMBO J. 8*, 2179–2188.

Schechter, I., & Berger, A. (1967) *Biochem. Biophys. Res. Commun. 27*, 157–162.

Sielecki, A. R., James, M. N. G., & Broughton, C. G. (1982) in *Computational Crystallography* (Sayre, D., Ed.) pp 409–419, Clarendon Press, Oxford.

Sielecki, A. R., Hayakawa, K., Fujinaga, M., Murphy, M. E. P., Fraser, M., Muir, A. K., Carilli, C. T., Lewicki, J. A., Baxter, J. D., & James, M. N. G. (1989) *Science 243*, 1346–1351.

Sielecki, A. R., Fedorov, A. A., Boodhoo, A., Andreeva, N. S., & James, M. N. G. (1990) *J. Mol. Biol. 214*, 143–170.

Street, I. P., Armstrong, C. R., & Withers, S. G. (1986) *Biochemistry 25*, 6021–6027.

Suguna, K., Padlan, E. A., Smith, C. W., Carlson, W. D., & Davies, D. R. (1987) *Proc. Natl. Acad. Sci. U.S.A. 84*, 7009–7013.

Thaisrivongs, S., Pals, D. T., Kati, W. M., Turner, S. R., Thomasco, L. M., & Watt, W. (1986) *J. Med. Chem. 29*, 2080–2087.

Workman, R. J., Burkitt, D. W. (1979) *Arch. Biochem. Biophys. 194*, 157–164.